

## Highlights

### **An Improved Metaheuristic Algorithm for On-site Workshop Availability Cost Problem**

Niloufar Mirzavand Boroujeni, Nima Moradi<sup>1</sup>

- A new model in project scheduling is presented: Multi-Mode On-Site Workshop Availability Cost Problem (MOSWACP).
- MOSWACP, formulated as a linear mathematical model, optimizes on-site workshops' lifetime and availability level, beginning time, and execution (operation) mode of activities.
- An Electron Radar Search Algorithm is developed and enhanced with problem-specific improvement operators.
- Comparative evaluation with SA, GA, and PSO is conducted alongside implementing the proposed model in a real case study.

---

<sup>1</sup>Corresponding author: Concordia Institute for Information and Systems Engineering, nima.moradi@mail.concordia.ca

# An Improved Metaheuristic Algorithm for On-site Workshop Availability Cost Problem

Niloufar Mirzavand Boroujeni<sup>a,c</sup>, Nima Moradi<sup>1b,c</sup>

<sup>a</sup>*University of Minnesota, Department of Industrial and Systems Engineering, Minneapolis, MN 55455, USA*

<sup>b</sup>*Concordia University, Concordia Institute for Information and Systems Engineering, Montreal, QC 1455, Canada*

<sup>c</sup>*These authors equally contributed to the present work and shared the first authorship.*

---

## Abstract

The Multi-mode Resource Availability Cost Problem (MRACP) optimizes resource availability to minimize usage costs and is a recent project scheduling problem variant. The Multi-Mode On-Site Workshop Availability Cost Problem (MOSWACP) extends MRACP by introducing spatial constraints for On-site Workshops (OSWs) at construction sites. MOSWACP aims to determine the optimal availability level, installation, and dismantling times for OSWs while scheduling activities within spatial and resource limitations. A novel Mixed-Integer Linear Programming (MILP) model is developed, and a metaheuristic algorithm, the Electron Radar Search Algorithm (ERSA), is proposed to solve large-scale instances. ERSA, enhanced with problem-specific operators, outperforms CPLEX in large instances and outperforms Simulated Annealing (SA), Genetic Algorithm (GA), and Particle Swarm Optimization (PSO). An actual case study demonstrated significant cost savings using the proposed model. The results and conclusions highlight the effectiveness of the ERSA approach in managing complex project scheduling challenges.

*Keywords:* Project scheduling, On-site workshop, Mathematical optimization, Resource availability cost problem, Electron radar search algorithm

---

## 1. Introduction

A Project Scheduling Problem (PSP) is a combinatorial optimization problem, finding activities' start and finish time under precedence relations constraints to minimize an objective, e.g., timespan and costs (Demeulemeester and Herroelen, 2006; Herroelen, 2005). PSP provides crucial assistance for various projects, like construction projects, to minimize the delays and unused resources caused by inappropriate scheduling. Also, poor project scope determination and design changes cause delays in over 50% of projects (Visual-Planning.com, 2020). Thus, PSP is a tool to reduce these delays and optimize the utilization of resources while minimizing the project's makespan and costs with a direct impact on time, cost, scope, and quality of the project outcome (GlobalKnowledge.com, 2020).

---

<sup>1</sup>Corresponding author: Concordia Institute for Information and Systems Engineering, nima.moradi@mail.concordia.ca



Figure 1: An on-site workshop for storage (ShelterLogic, 2022)

Moreover, resource unavailability, delay of material procurement, space capacity limitation, and project deadline are preliminary sources of complexity for PSP. Variants of PSP are introduced in the literature to involve these sources of complexities. For example, Resource-Constrained PSP (RCPSP) involves resource unavailability, which imposes a limitation on the resource of each activity at different time frames (Brucker et al., 1999; Herroelen et al., 1998; Pellerin et al., 2020; Hartmann and Briskorn, 2022). Time-Constrained PSP (TCPSP) (Guldemond et al., 2008), a.k.a. Resource Investment Problem (RIP) (Drexl and Kimms, 2001), is another variant of PSP, which focuses on the project’s deadline at minimized resource utilization cost. RIP can also be referred to as the Resource Availability Cost Problem (RACP), which extends RIP to penalize the project’s delay or tardiness. RACP minimizes the penalties for project deadline violations instead of minimizing project makespan.

Furthermore, the resources in the RACP can be categorized into (non)renewable, doubly constrained, and partially (non)renewable. Renewable resources such as labor, machines, and equipment have limited usage over periods and are replenished for the following periods. In contrast, non-renewable resources, such as money and raw materials, are consumed and not replenished over the planning horizon. Doubly-constrained resources such as periodic budgets are renewable from one period to another but not at each period. Moreover, Partially (non)renewable resources are available during specific periods, and the project activities that require such resources should utilize them only during their availability (Böttcher et al., 1999). An On-Site Workshop (OSW) is a resource that is partially (non)renewable, involving spatial constraints with a pre-defined lifespan from installation to dismantling. We illustrate an example of OSW in Fig. 1, a temporary workshop similar to a garage, protecting project materials vulnerable to heat and rain. OSWs are installed once a project activity requires them and are dismantled upon completion of that activity (ShelterLogic, 2022). They effectively reduce the project’s costs and makespan by distributing the resources efficiently throughout a project construction or production site considering the project’s constraints.

This paper introduces the Multi-Mode On-Site Workshop Availability Cost Problem (MOSWACP), in which at least a task (activity) can be undertaken in multiple modes to extend RACP constrained to OSWs’ spatial capacity and lifetime. The primary motivation for introducing this problem is that the assumption of resources without spatial and lifetime conditions will result in non-optimal (e.g., sub-optimal) solutions. So, by considering the spatial and lifetime-constrained resources, MOSWACP finds more realistic scheduling of activities and resources (e.g., OSWs) than the existing project scheduling-related problems by

incorporating real-world aspects of resources and constrained spatial capacity of the project's site. The contributions of the present work are presented as follows:

- Addressing a novel construction project problem, multi-mode resource availability cost problem, considering spatial and installation/dismantling times of resources (e.g., OSWs), project site's spatial capacity, and PSP-related constraints.
- Formulating the addressed problem by a novel MILP model with linear constraints.
- Proposing an efficient problem-specific ERSA metaheuristic, comparing with an exact solver and three existing metaheuristics on a new benchmark.
- Conducting the comparative study, sensitivity analysis, and a real case study to show the applicability of the proposed model in real situations.

The paper is structured as follows: the related literature is reviewed in Section 2. Section 3 presents a Mixed-integer Linear Programming (MILP) model for a relatively small-scale MOSWACP. To solve large-scale MOSWACPs, an Electron Radar Search Algorithm (ERSA)-based metaheuristic is proposed in Section 4. Then, the performance of the proposed metaheuristic is compared with a commercial exact solver and existing metaheuristics while conducting a real case study to show the practicability of the proposed model in Section 5. Finally, conclusions, future directions, and model limitations are discussed in Section 6.

## 2. Literature Review

There are several extensions of Resource-Constrained Project Scheduling Problem (RCPSP) in the literature: (a) Multi-Mode RCPSP (MRCPSPP) (Alcaraz et al., 2003), that finds optimal execution mode for each activity; (b) Preemptive MRCPSPP (Van Peteghem and Vanhoucke, 2010), which presumes activities could be split or preempted during the project; (c) RCPSP with flexible resource profiles (Naber and Kolisch, 2014) in which resource usage of activities can be shifted from one period to another; (d) RCPSP with uncertain resource availabilities (Lambrechts et al., 2008); (e) Multi-objective RCPSP (Viana and de Sousa, 2000) which minimizes the project duration, delay of activities, and resource capacity violation; (f) Stochastic RCPSP (Deblaere et al., 2011) that involves the uncertain duration of project activities; and (g) MRCPSPP with generalized precedence relations (De Reyck and Herroelen, 1999) which takes care of a range of time intervals between the start and finish times of the activities.

Furthermore, TCPSP, also known as RIP (Drexl and Kimms, 2001), optimizes the availability of resources to minimize resource usage costs while satisfying project deadlines. Several extensions of RIP are introduced in the literature as follows.

- RIP with tardiness penalty (Shadrokh and Kianfar, 2007), which penalizes tardiness of projects.
- RIP with discounted cash flows (Najafi and Niaki, 2006), which optimizes the net present value of the project cash flows.

- RIP with discounted cash flows and generalized precedence relations (Najafi et al., 2009).
- RIP with time windows (Lu et al., 2019), in which the periods of resource availability are variant.
- RIP with quantity discount in ordering materials (Shahsavar et al., 2018).
- RIP with discounted cash flows and generalized precedence relations under inflation (Shahsavar et al., 2010).
- Multi-Mode RIP (MRIP) (Hsu and Kim, 2005; Gerhards and Stürck, 2018) in which at least a task can be undertaken in several modes.
- Preemptive multi-skilled RIP (Javanmard et al., 2017) minimizes the total recruitment cost in the presence of multi-skilled workers.
- Uncertain Multi-objective MRIP (Subulan, 2020) in which the completion time of activities and availability of renewable resources are uncertain.

RACP (Zhu et al., 2017) is another extension of RIP where the tardiness of the project completion time is associated with a penalty. The RACP solvers can be classified into three groups: exact, heuristic, and metaheuristic. Hybrid method with branching scheme (Rodrigues and Yamashita, 2010), Constraint Programming (CP) (Kreter et al., 2018), and Modified Minimum Bounding Algorithm (MMBA) (Rodrigues and Yamashita, 2015) are among the exact solvers. However, since the exact solvers might be computationally expensive, some heuristic algorithms are developed to solve RACP (Peteghem and Vanhoucke, 2015; Zhu et al., 2017; Rose et al., 2016; Hsu and Kim, 2005; Su et al., 2018; Chen et al., 2012). Also, for RACP with relatively complicated guidelines, metaheuristics are proposed such as Scatter Search (SS) (Yamashita et al., 2006; Meng et al., 2016), SS with a multi-start heuristic (Yamashita et al., 2007), Artificial Immune System (AIS) (Van Peteghem and Vanhoucke, 2013), path relinking with Genetic Algorithm (GA) (Ranjbar et al., 2008), pseudo Particle Swarm Optimization (PSO) (Qi et al., 2014), and Invasive Weed Optimization (IWO) (Van Peteghem and Vanhoucke, 2012).

In addition to the solvers to RACP, several extensions of RACP model are studied in the literature including Multi-Mode RACP (MRACP) (Afshar-Nadjafi, 2014a; Qi et al., 2014; Yamashita et al., 2009), RACP with rental resources (Afshar-Nadjafi et al., 2017), RACP with tardiness (Su et al., 2018), multi-objective stochastic RACP (Arjmand et al., 2020), RACP with time-dependant resource cost (Afshar-Nadjafi, 2014b), and RACP with a limited lifetime of resources (Afshar-Nadjafi, 2014a), from recruitment (installation) to release (dismantling) periods.

In construction or production project scheduling problems, OSWs are partially renewable resources that require physical space, which is limited in construction sites and can be bottlenecks for project completion. We take care of these spatial limitations with efficient OSW installation and dismantling. To this end, we involve OSW in RACP to propose a novel extension to RACP. Solving the project scheduling problems with spatial storage limitations may require expensive computational resources. Metaheuristic algorithms are developed

in the literature to mitigate extensive computations. For instance, (Moradi and Shadrokh, 2019), unlike the previous models with single warehouse and unlimited storage capacity, take into account several warehouses with restricted capacity throughout the planning horizon.. They developed a Simulated Annealing algorithm to solve the model. Moreover, (Zhang and Cui, 2021) examined the Project Scheduling and Material Ordering Problem (PSMOP) while accounting for limitation of the storage capacity. The model they developed minimizes the project makespan, stock of materials, ordering costs, and secondary expenses by selecting the optimal activities’ timeline, along with determining the timing and amount of material orders. They also presented an efficient non-dominated sorting GA algorithm to optimize large-sized problems. Moreover, (Tian et al., 2023) addressed an integrated PSMOP and RCPSP with Limited Storage Space, concentrating on scheduling activities and ordering materials while adhering to storage limitations. They introduced a two-layer heuristic algorithm to solve this model effectively. The problem discussed in the paper, differs from RCPSP-MPS since it involves utilizing esources with partial renewability (or nonrenewability), concurrent activities, and OSWs.

We introduce a problem in project scheduling, MOSWACP, which determines the optimal lifespan and availability threshold of OSWs and the initiation time and execution mode of each activity. Then, we adopt a MILP model for MOSWACP to find optimal solutions for instances of relatively smaller size of MOSWACP and propose an ERSA-based metaheuristic to solve large-scale MOSWACP. Our proposed metaheuristic algorithm enhances ERSA with problem-specific improvement rules, outperforming existing SA, GA, and PSO algorithms. Our research method involves a literature review to understand the problem domain, identifies research gaps, helps adopt a linear mathematical model as a theoretical foundation, and proposes an ERSA metaheuristic to enhance efficiency and performance evaluation by generating different problem instances, including custom-generated benchmarks, and executing tests.

### 3. Multi-Mode On-Site Workshop Availability Cost Problem

To formulate MOSWACP, we presume: (1) A single OSW cannot be divided into distinct components; (2) The construction site has restricted space; (3) Each OSW has a unique functionality; (4) The activities have fixed duration times; (5) The activities have multiple execution modes; (6) Each OSW occupies a fixed physical space; (7) Precedence relationships are the finish-to-start (FS) kind; (8) Each OSW is installed at the starting time of the first activity dependent on the OSW. Also, each OSW is dismantled at the finish time of the last activity dependent on the OSW; (9) Tardiness is not permitted; (10) The activities are non-preemptive; and (11) The OSWs are partially (non)renewable resources with pre-determined lifetimes and sizes.

OSWs significantly influence the construction projects’ completion time, cost, and quality. However, due to limited physical space in construction sites, we may be unable to install OSWs at our convenience. Physical space limitations in construction sites may significantly influence the project’s timeline. Let’s take a construction project with 5 activities each of which with a single mode of execution, and two OSWs as an example, illustrated by an activity-on-node (AON) network in Fig. 2. We denote the space that the OSW  $k$  and activity  $i$  require by  $r_{ik}$  and add two dummy activities, 0 and 6. Also, we specify the duration of each

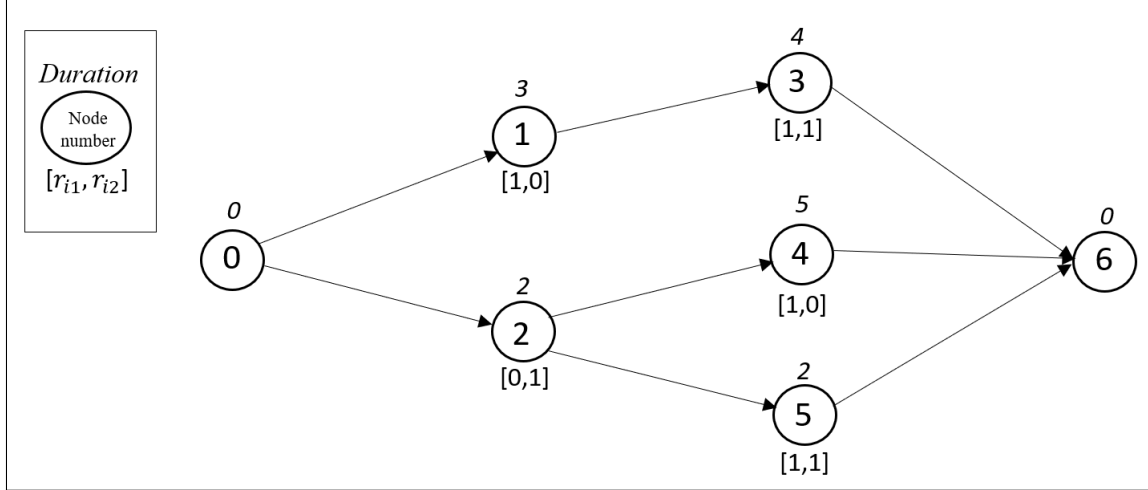
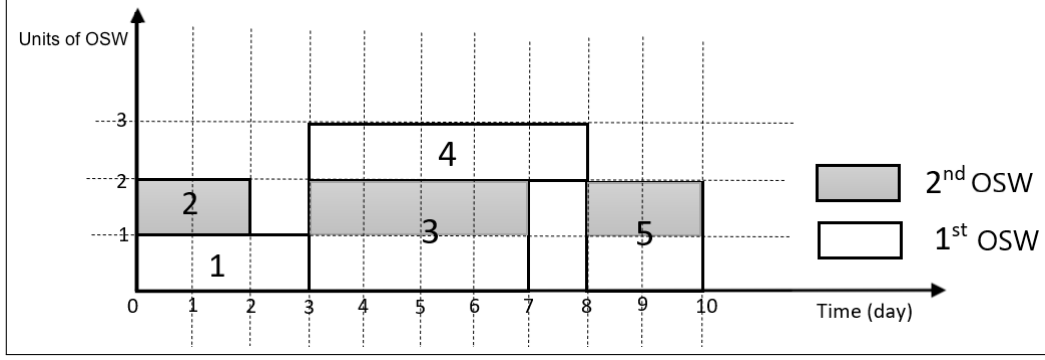


Figure 2: The example of an AON network

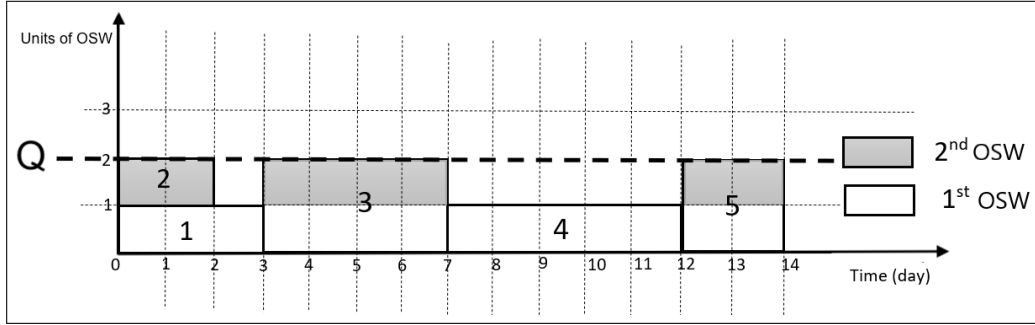
activity right above each activity node in this figure and presume all activities are single-mode types, and precedent relationships are finish-to-start types. A feasible scheduling solution for this project with unlimited and limited physical space is shown in Fig. 3, illustrating the activities' start and finish times and OSW utilization. Even though the project's duration is 10 days, with limited physical space, imposing a limitation on the physical space delays the project by 40%.

We present MOSWACP as a directed graph of the activity-on-node network,  $G = (V, E)$ , where  $V = \{0, 1, \dots, N + 1\}$  is the set of activities (nodes) and  $E$  is the set of finish-to-start precedence relationship between activities.  $V_0$  and  $V_{N+1}$  are dummy activities as the initial and terminal nodes, respectively. The activity  $j \in V \setminus \{0, N + 1\}$  with the execution mode,  $i \in m_j$ , where  $m_j$  is the set of possible modes of execution for activity  $j$ , with fixed time period,  $d_{ji}$ . Also, the activity,  $j \in J$ , with the execution mode,  $i \in m_j$ , demands a designated physical area,  $r_{jik}$ , at every OSW,  $k \in K$ . The precedent activities of activity  $j \in J$  are given by  $P_j$ . The site has a limited area,  $Q$ , and the cost of utilizing an OSW is  $C_k$ . The project has a deadline of  $T_{max}$ , and the planning horizon is  $T$ .  $x_{it}$  is a binary decision variable which equals 1 if activity  $i \in J$  starts at period  $t = 0, 1, \dots, T$  and equals 0 otherwise. Also,  $z_{ij}$  is a binary decision variable that takes 1 if activity  $i \in J$  gets executed on mode  $j \in m_i$ , and it equals 0 otherwise.  $y_{kt}$  is a binary decision variable and equals one if OSW  $k \in K$  is installed at period  $t = 0, 1, \dots, T$  and equals 0 otherwise.  $R_k$  denotes the OSW  $k$ 's level of availability, where  $k \in K$ .

Using the notations shown in Table 1, the mathematical programming formulation of MOSWACP, adapted from (Moradi et al., 2023), is presented as Model (1)-(10). The objective function (1) minimizes the cost of OSWs' usage. Constraint (2) guarantees the precedence relationships between the activities. Constraint (3) ensures the occupied area of each OSW does not exceed its level of availability. Constraint (4) limits the construction site's physical space capacity. Constraint (5) ensures when an OSW-required activity is started, the corresponding OSW is installed and remains active until the activity is finished. Constraint (6) imposes a deadline on the project. Constraint (7) ensures that only one execution mode is selected for each activity. By constraint (8), each activity starts only once. Con-



(a) A feasible schedule with unlimited physical space



(b) A feasible schedule with a limited physical space

Figure 3: The comparison of feasible schedules with (a) limited and (b) unlimited physical space to the AON network in Fig. 2

straint (9) sets the initial activity's start time. Finally, the domain of the decision variables is represented by constraint (10).

$$\min . \sum_{K \in k} C_k R_k, \quad (1)$$

s.t.

$$\sum_{t=0}^T tx_{it} \geq \sum_{u \in m_i} z_{ju} d_{ju} + \sum_{t=0}^T tx_{jt}, \quad \forall i \in J, \forall j \in P_i \quad (2)$$

$$\sum_{i \in J} \sum_{j \in m_i} z_{ij} r_{ijk} y_{kt} \leq R_k, \quad \forall k \in K, t = \{0, 1, \dots, T\} \quad (3)$$

$$\sum_{k \in K} R_k y_{kt} \leq Q, \quad t = \{0, 1, \dots, T\} \quad (4)$$

$$tx_{it} + \sum_{j \in m_i} d_{ij} z_{ij} - 1 \leq \sum_{l=0}^T y_{kl}, \quad \forall i \in J, \forall k \in K, t = \{0, 1, \dots, T\} \quad (5)$$

$$\sum_{t=0}^T tx_{n+1,t} \leq T_{max}, \quad t = \{0, 1, \dots, T\} \quad (6)$$

$$\sum_{j \in m_i} z_{ij} = 1, \quad \forall i \in J \quad (7)$$

$$\sum_{t=0}^T x_{it} = 1, \quad \forall i \in J \quad (8)$$

$$x_{00} = 1, \quad (9)$$

$$x_{it}, z_{ij}, y_{kt} \in \{0, 1\}, \quad \forall i \in J, \forall j \in m_i, \forall k \in K, t = \{0, 1, \dots, T\} \quad (10)$$

The Model (1)-(10) is a nonlinear optimization model with high computational complexity. To solve the problem with commercial solvers, such as Gurobi or CPLEX (CPLEX,



Table 1: Notations of the model

Notation	Description
<b>Sets</b>	
$J$	Activities excluding initial and terminal (dummy) activities
$m_j$	Possible execution modes of activity $j \in J$
$K$	Available OSWs
$P_j$	Precedent activities of activity $j \in J$
<b>Parameters</b>	
$N$	Number of project (non-dummy) activities
$d_{ji}$	Duration of activity $j$ executed on mode $i \in m_j$
$r_{jik}$	The space occupied by activity $j \in J$ on execution mode $i \in m_j$ in OSW $k \in K$
$Q$	The construction site's physical area
$C_k$	Usage cost of OSW $k \in K$
$T$	Planning horizon
$T_{max}$	Project deadline
<b>Decision variables</b>	
$x_{it}$	= 1 if activity $i \in J$ starts at time $t = \{0, 1, \dots, T\}$ ; 0 otherwise
$z_{ij}$	= 1 if activity $i \in J$ is executed by the mode $j \in m_i$ ; 0 otherwise
$y_{kt}$	= 1 if the OSW $k \in K$ is installed at time $t = \{0, 1, \dots, T\}$ ; 0 otherwise
$R_k$	Availability level of OSW $k \in K$

2023), we linearize the model by linearizing constraints (3) and (4).

### 3.1. Linearization of constraint (3)

We define a new binary decision variable,  $y'_{ijkt}$ . It equals 1 if activity  $i \in J$  with the execution mode  $j \in m_i$  occupies the OSW  $k \in K$  at the period  $t = \{0, 1, \dots, T\}$ , otherwise it equals 0. Accordingly, we replace constraint (3) with constraints (11)-(13).

$$\sum_{i \in J} \sum_{j \in m_i} r_{ijk} y'_{ijkt} \leq R_k, \quad \forall k \in K, t = \{0, 1, \dots, T\} \quad (11)$$

$$y'_{ijkt} + 1 \geq z_{ij} + y_{kt}, \quad \forall i \in J, \forall j \in m_i, \forall k \in K, t = \{0, 1, \dots, T\} \quad (12)$$

$$y'_{ijkt} \leq \alpha(z_{ij} + y_{kt}), \quad \forall i \in J, \forall j \in m_i, \forall k \in K, t = \{0, 1, \dots, T\} \quad (13)$$

Where  $\alpha$  is an arbitrary constant parameter such that  $0 < \alpha < 1$ .

### 3.2. Linearization of constraint (4)

We defined a new decision variable,  $R'_{kt}$ , as the availability level of OSW  $k \in K$  at period  $t = \{0, 1, \dots, T\}$ . Then, we replace the constraint (4) with constraints (14)-(17).

$$\sum_{k \in K} R'_{kt} \leq Q, \quad t = \{0, 1, \dots, T\} \quad (14)$$

$$0 \leq R'_{kt} \leq R_k, \quad \forall k \in K, t = \{0, 1, \dots, T\} \quad (15)$$

$$R'_{kt} \leq M y_{kt}, \quad \forall k \in K, t = \{0, 1, \dots, T\} \quad (16)$$

$$R'_{kt} \geq R_k - M(1 - y_{kt}), \quad \forall k \in K, t = \{0, 1, \dots, T\} \quad (17)$$

Where  $M$  is a big constant parameter, such that  $0 \leq R_k \leq M, \forall k \in K$ .

Finally, we reformulate the adopted nonlinear MIP (1)-(10) to a linear MIP (1), (2), (5)-(17), (18).

$$\begin{aligned}
& \min. \quad \text{Objective function (1),} \\
& \text{s.t.} \\
& \quad \text{Constraints (2), (5) - (17),} \\
& \quad y'_{ijkt}, R'_{kt} \in \{0, 1\}, \quad \forall i \in J, \forall j \in m_i, \forall k \in K, t = \{0, 1, \dots, T\}.
\end{aligned} \tag{18}$$

The adopted MIP model for MOSWACP has  $T\bar{K}m'$  decision variables and  $n' + T\bar{K}m'$  constraints.  $\bar{K}$ ,  $m'$ , and  $n'$  are the total number of available OSWs, the total number of execution modes, and the total number of precedent activities, respectively. MOSWACP extends the Multi-Mode Resource Investment Problem with tardiness (MRIPT). Since MRIPT is NP-hard (Gerhards, 2020), and MOSWACP can be reduced to MRIPT, the MOSWACP is NP-hard, too. The existing commercial solvers cannot solve a large-scale MOSWACP within a reasonable time. Thus, we developed the metaheuristic algorithm, Electron Radar Search Algorithm (ERSA), to generate solutions for large-scale MOSWACPs.

#### 4. Electron Radar Search Algorithm for MOSWACP

ERSA was first introduced by (Rahmanzadeh and Pishvae, 2020), which mimics the natural behavior of electric flow when the electrons are in a gas, liquid, or pooplid environment. When the voltage between the anode and cathode increases, the electrons emit from a lower to a higher potential. In this situation, the electrons emit through a way by which they encounter the least resistance in the environment. To evaluate the surrounding environment and find the path with less resistance, the electrons use a radar mechanism to search the environment for an efficient path. ERSA finds the best solution in 95% of the benchmark functions (Rahmanzadeh and Pishvae, 2020), so we re-design it to comply with our proposed MOSWACP and solve it. We present the pseudo-code of ERSA in Alg. 1. In this pseudo-code,  $\beta$  controls the balance between exploration and exploitation,  $E_n^0$  is the number of electrons for each initial solution,  $CV$  is the critical value,  $r$  is the searching radius for each solution, and  $M$  is the number of random points chosen for the local search at each iteration,  $t$ .

##### 4.1. Solution representation

We built a  $2n + 3\bar{K}$ -dimensional vector to represent the solution space for the MOSWACP problem as

$$\{S_1, \dots, S_n, SW_1, \dots, SW_{\bar{K}}, FW_1, \dots, FW_{\bar{K}}, M_1, \dots, M_n, R_1, \dots, R_{\bar{K}}\}.$$

where  $n$  denotes the total number of activities, and  $\bar{K}$  represents total OSWs. The solution representation in the proposed ERSA is a  $(2n + 3\bar{K})$ -dimensional vector, in which  $\{S_1, \dots, S_n\}$ ,  $\{SW_1, \dots, SW_{\bar{K}}\}$ ,  $\{FW_1, \dots, FW_{\bar{K}}\}$ ,  $\{M_1, \dots, M_n\}$ , and  $\{R_1, \dots, R_{\bar{K}}\}$  are

---

**Algorithm 1** The pseudo-code of ERSA (Rahmanzadeh and Pishvaei, 2020)

---

```

1: Start
2: End
3: Inputs: Initial population of streamers ( $N$ ), parameters  $\beta$ ,  $E_n^0$ ,  $CV$ ,  $r$ ,  $M$ , and  $t = 0$ 
4: while The number of existing streamers is greater than zero do
5:   for each streamer do
6:     if Eliminating condition is satisfied then
7:       Eliminate streamer and go to the next streamer
8:     else if Forking condition is satisfied then
9:       Create a new streamer randomly and update the population of streamers
10:    end if
11:    Update streamer position and save the best objective function
12:  end for
13: end while
14: Display the best objective function

```

---

the activities' start time, the installation time of the OSWs, the dismantling duration of OSWs, the execution mode selected for activities, and the level of OSWs' availability, in corresponding order.

#### 4.2. Initial population generation

The initial population set must constitute a feasible solution for MOSWACP. First, we find  $R_k, k \in K$ , through the allocation of a randomly generated integer that exceeds  $\max_{i \in J, j \in m_i} \{r_{ijk}\}$ . Second, we find  $M_i (i \in J)$  by selecting a random integer from set  $m_i$ , which is the execution mode of the activity  $i$ . Third, we use Alg. 2 to determine the initiation time of the activities. Finally,  $SW_k$  and  $FW_k, k \in K$  are determined based on the activities that require OSW  $k \in K$  to begin, as Eq. (19).

$$SW_k = \min_{i: \exists j \in m_i, r_{ijk} \neq 0} \{S_i\}, \quad FW_k = \max_{i: \exists j \in m_i, r_{ijk} \neq 0} \{S_i + d_{ij}\} \quad (19)$$

#### 4.3. Improvement-based local search

ERSA employs an improvement-based local search to create the neighboring solution by practical crossover and mutation operators. Then, it is improved by applying three efficient improvement rules represented in Table 2. The inputs and outputs of the crossover operator are 2 solutions, each of which known as parent and offspring solutions. We presume  $Sol_1$  and  $Sol_2$  are parent solutions as follows.

$$Sol_1 : \{S_1^1, \dots, S_n^1, SW_1^1, \dots, SW_K^1, FW_1^1, \dots, FW_K^1, M_1^1, \dots, M_n^1, R_1^1, \dots, R_K^1\}.$$

$$Sol_2 : \{S_1^2, \dots, S_n^2, SW_1^2, \dots, SW_K^2, FW_1^2, \dots, FW_K^2, M_1^2, \dots, M_n^2, R_1^2, \dots, R_K^2\}.$$

We determine a new point based on the crossover point of a single-point crossover,  $C_p$ . The crossover then takes place at this point, producing the offspring solutions,  $Sol_3$  and  $Sol_4$ , as described below.

---

**Algorithm 2** Feasible schedule generator for project activities
 

---

```

1: Start
2: Set  $S_0 = 0$ 
3: while The scheduling is not finished do
4:   Choose the next activity in the set  $\{S_1, \dots, S_n\}$ 
5:   for  $i = 1$  to  $n$  do
6:     Set  $S_i = \max_{u \in P_i} \{S_u + d_{uj}\}$  for  $j = M_u \triangleright P_i$  is the set of precedent activities of
       activity  $i$ ,  $M_u$  has already been determined in the chromosome
7:      $R_k$ 
8:     if  $R_k \leq Q$  then
9:        $R_k \leftarrow R_k + r_{ijk}$  for  $j = M_i$   $\triangleright$  Updating  $R_k$ 
10:    end if
11:  end for
12: end while
13: Return  $S_1, \dots, S_n$ 
14: End

```

---

$$Sol_1 : \{S_1^1, \dots, S_n^1, SW_1^1, \dots, SW_{\bar{K}}^1 \otimes, FW_1^1, \dots, FW_{\bar{K}}^1, M_1^1, \dots, M_n^1, R_1^1, \dots, R_{\bar{K}}^1\}$$

$$Sol_2 : \{S_1^2, \dots, S_n^2, SW_1^2, \dots, SW_{\bar{K}}^2 \otimes, FW_1^2, \dots, FW_{\bar{K}}^2, M_1^2, \dots, M_n^2, R_1^2, \dots, R_{\bar{K}}^2\}$$

↓

$$Sol_3 : \{S_1^1, \dots, S_n^1, SW_1^1, \dots, SW_{\bar{K}}^1 \otimes, FW_1^2, \dots, FW_{\bar{K}}^2, M_1^2, \dots, M_n^2, R_1^2, \dots, R_{\bar{K}}^2\}$$

$$Sol_4 : \{S_1^2, \dots, S_n^2, SW_1^2, \dots, SW_{\bar{K}}^2 \otimes, FW_1^1, \dots, FW_{\bar{K}}^1, M_1^1, \dots, M_n^1, R_1^1, \dots, R_{\bar{K}}^1\}$$

With the symbol  $\otimes$  and  $C_p = n + \bar{K}$ , crossover point is positioned between  $n + \bar{K}$  and  $n + \bar{K} + 1$ .

Since the offspring solutions might be infeasible, we designed a crossover operator to transform an infeasible solution to a feasible one. If the crossover modify the beginning time of the activities, we call Alg. 2 to repair the infeasible schedule. Additionally, if the crossover alters the OSW schedule, we transform the infeasible schedule into a feasible one by Eq. (19). Moreover, in case the crossover shifts the execution mode of an activity, we update the schedule of the activities and OSW according to the new execution modes by Alg. 2. Finally, in case the crossover modifies the OSWs' availability level, we update the schedule of OSWs and activities based off of the new availability levels using Alg. 2.

The mutation operator takes one solution, and creates a mutated solution. The number of bits (elements) mutated in each solution is determined by  $r_m$ . Let's take the solution,  $Sol_1$ , to mutate as follows.

$$Sol_1 : \{S_1^1, \dots, S_n^1, SW_1^1, \dots, SW_{\bar{K}}^1, FW_1^1, \dots, FW_{\bar{K}}^1, M_1^1, \dots, M_n^1, R_1^1, \dots, R_{\bar{K}}^1\}$$

We mutate the elements  $n$  and  $n + \bar{K}$ , such that  $r_m = 2$ . The new solution becomes as follows.

$$\{S_1^1, \dots, S_n^1, SW_1^1, \dots, SW_K^1, FW_1^1, \dots, FW_K^1, M_1^1, \dots, M_n^1, R_1^1, \dots, R_K^1\}$$

Where  $S_n^1$  and  $SW_K^1$  are the new elements.

The solution may become infeasible by mutation. In that case, we use Alg. 2 to convert infeasible solutions into feasible solutions. If the mutation changes the activity schedule, we convert the activity's start times to satisfy precedence relationships and the space capacity constraints. Also, if the mutation operator changes the installation or dismantling times of the OSW, we modify the corresponding installation or dismantling times to maintain the feasibility of the activities schedule. Likewise, if the mutation operator modifies the availability level of an OSW, we modify the corresponding OSW's availability level to maintain the feasibility of the schedule and space capacity. Finally, if the mutation operator shifts the execution modes, we switch that activity to support the feasibility of activities' schedules and space capacity. As the fitness function involves the cost of OSWs utilization, we calculate total usage cost by  $\sum_{k \in K} R_k C_k$ .

The proposed ERSA in this study incorporates three MOSWACP-specific improvement operators, as shown earlier in Table 2.

Table 2: Improvement rules in the proposed ERSA

Improvement rule	Description
Switching the execution mode, $IR_1$	Switch the execution mode of activities while maintaining the feasibility of solutions as well as improving the value of the objective function
Rescheduling activities, $IR_2$	Reschedule the activity's start time based on its float time and improve the values of the objective function at the same time
Regularizing OSWs' level of availability, $IR_3$	Regularize the availability of an OSW without violating the physical space limitation an OSW takes

The first improvement operator, denoted as  $IR_1$ , focuses on altering the activities' mode of execution to achieve two primary goals: (i) Reduce the project's makespan by parallelizing activities, and (ii) Optimize the utilization of OSWs and avoid the physical space violation.

Let's take an example of a construction site, shown in Fig. 4, with 5 OSWs, in which the activity 1 utilizes the OSWs  $\{1, 4, 5\}$ , activity 2 utilizes  $\{1, 2, 3\}$ , and activity 3 utilizes  $\{3, 4\}$ . The improvement operator,  $IR_1$ , switches the activity's execution mode 1 from mode 1 to mode 2. In this case, the second execution mode requires activity 1 to take relatively more space in workshop 4, while not demanding a space in OSW 5, as illustrated in Fig. 5. Consequently, we can execute activity 4 concurrent with activities 1, 2, and 3 due to the precedence relationships outlined in Fig. 4. Activity 4 occupies workshop 6 only so that our adjustment does not violate the physical space capacity. In this example, we can reduce the project duration by effectively parallelizing 4 activities without violating the constraints.

The second improvement operator, denoted as  $IR_2$ , rearranges the scheduling of activities based on their float times and reduces the project's makespan, consistent with precedence relationships and the area's constrained capacity. To illustrate the improvement operator  $IR_2$ , let's take the scenario depicted in Fig. 4 as an example, where the duration of activities

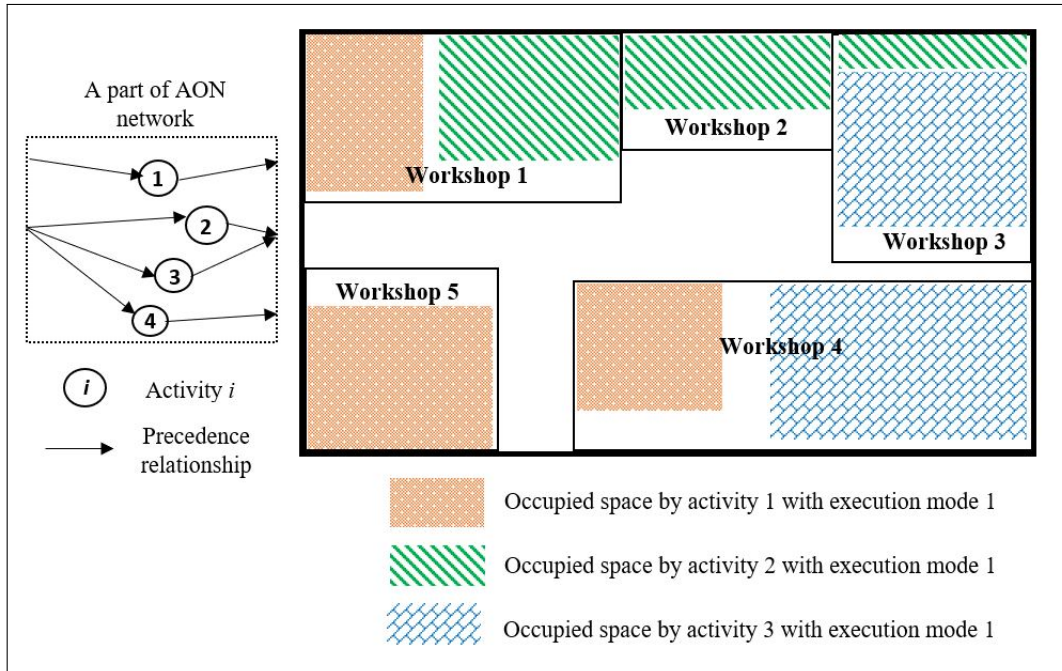


Figure 4: A construction site with 5 OSWs and the corresponding project AON network, where activity 1 is executed on mode 1

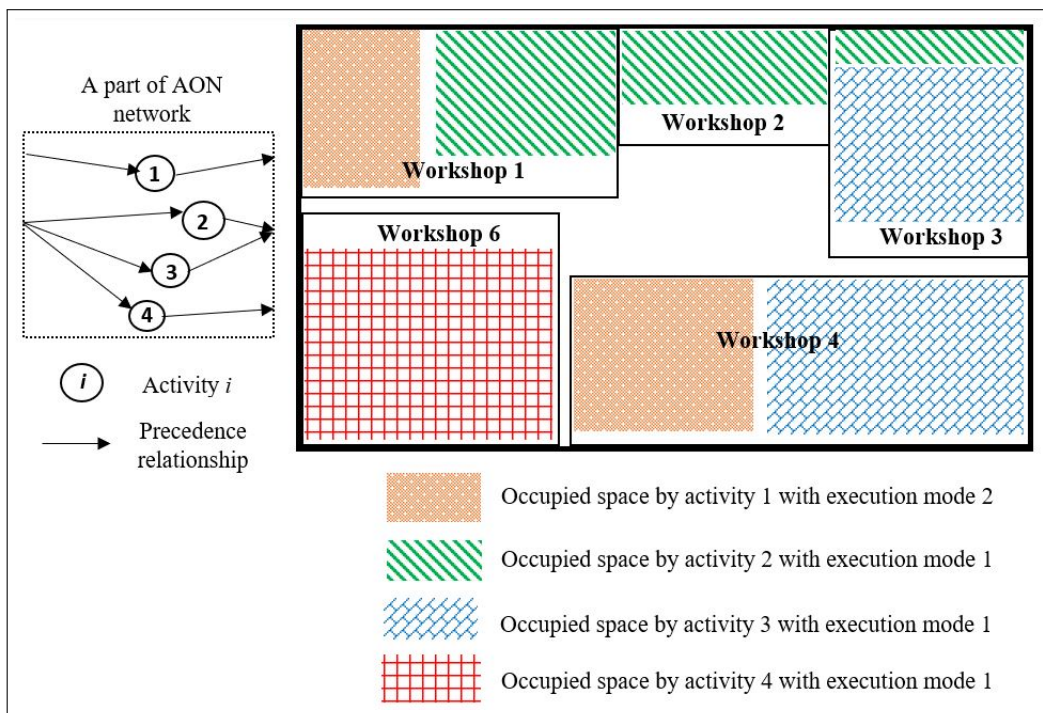


Figure 5: A construction site with 5 OSWs and the corresponding project AON network, where the execution mode of activity 1 is switched from mode 1 to mode 2 by  $IR_1$

1 – 4 are 3, 4, 3, and 6 periods, respectively. Due to the limited area at the construction site, activity 4 cannot commence until, say, one of the activities 1 – 3 is complete. A feasible

schedule for this project is shown in Fig. 6. In this example, activity 1 is not a direct successor of 2 or 3. In such cases, the improvement operator,  $IR_2$ , shifts the activity's start time 1 from 0 to 3; see Fig. 7. This rule reduces the overall project duration by 33%; see Fig. 6, and Fig. 7.

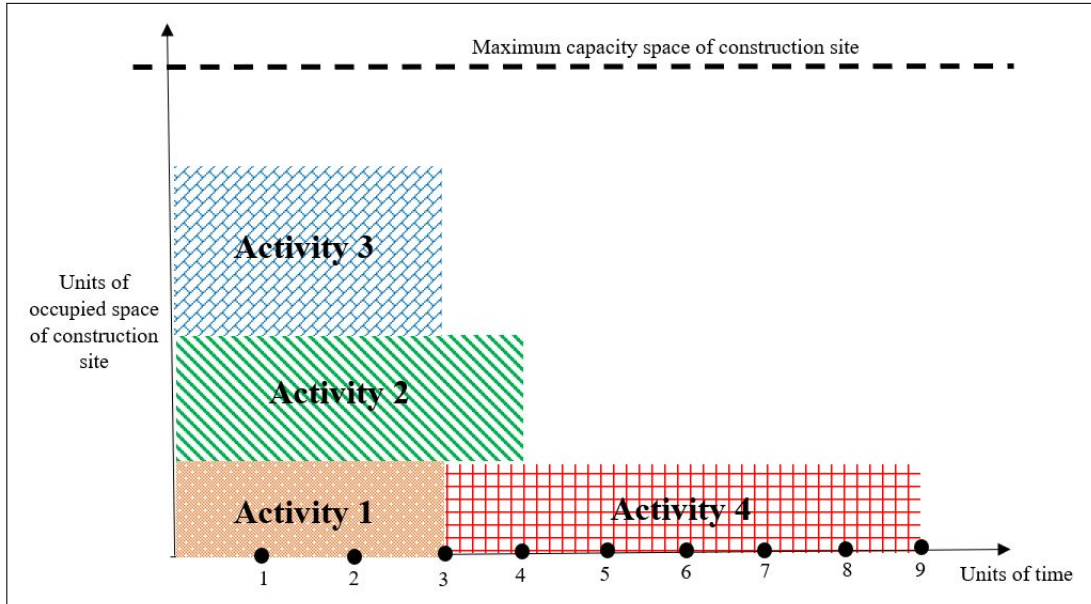


Figure 6: Activities schedule when activity 1 starts at time zero

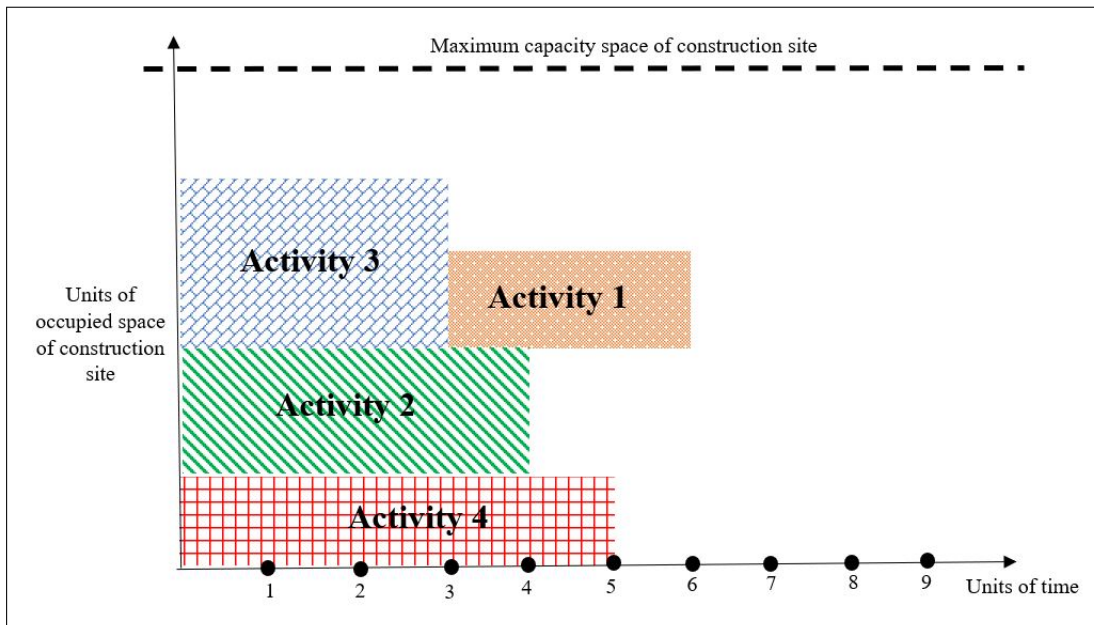


Figure 7: Activities schedule when activity one is rescheduled to start at time three by  $IR_2$

The improvement operator,  $IR_3$ , optimizes the size or availability level of OSWs to incorporate additional workshops on the site. Let's take the construction site depicted in Fig.

4 as an example. The improvement operator,  $IR_3$ , reduces OSWs' availability level and maintains the demanded physical space of activities in them. By resizing the workshop(s), we add space to the site and install an additional OSW, as Workshop 6 in Fig. 8. This adjustment facilitates the concurrent execution of more activities and ultimately improves the project schedules and allocation of resources efficiently.

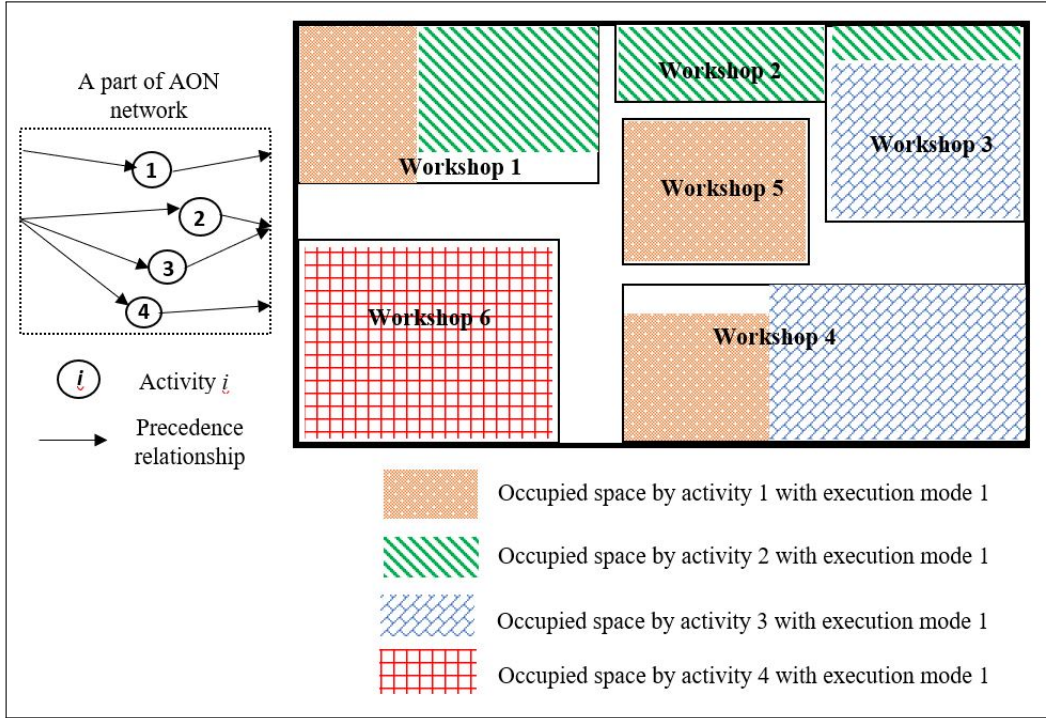


Figure 8: The construction site, occupied with 6 OSWs while the size of each OSW is regularized by  $IR_3$

## 5. Computational Results

In this section, we solve the MOSWACP with MIP solver, ERSA, and well-known meta-heuristics, including SA (Moradi et al., 2022), GA (Moradi et al., 2023), and PSO (Kayvanfar et al., 2023). Also, we compare the performance of the solvers. We solve the MIP model using the CPLEX Application Programming Interface (API) in Python and code the ERSA in C++ on a 1.60 GHz Core i5 processor with 16GB of RAM. The parameters of MOSWACP are close to the well-known MRCPSP (Alcaraz et al., 2003). To generate the instances for MOSWACP, we add the utilization cost of each OSW,  $C_k$ , and its corresponding demanding area utilized with execution mode  $i$ ,  $r_{jik}$  of activity  $j$ , to the MMRCPSP instances.

### 5.1. Instance generation for MOSWACP

In this section, we explain how we involve novel parameters used in the literature to generate diverse instances of MOSWACP. The parameters for MOSWACP closely resemble those of the well-known MMRCPSP (Drexel and Gruenewald, 1993). To create MOSWACP



instances, we involve  $C_k$  and  $r_{jik}$  in MMRCPS library<sup>2</sup>, which represent the usage cost of the OSW,  $k$ , and the space occupied by activity,  $j$ , with execution mode,  $i$ , respectively. We selected the instances,  $C15$ ,  $C21$ ,  $J10$ ,  $J12$ ,  $J14$ ,  $J16$ ,  $J18$ ,  $J20$ ,  $M2$ , and  $R3$ , from this library. We evaluate how the problem responds to the parameter variations using 16 different instances of  $J10$ . Subsequently, we incrementally range the parameter  $r_{jik}$  from 0 to 13, with other parameters fixed. Similarly, incrementally, we set the parameter  $C_k$  to several different values from  $\{10, 20, 30, 50, 100\}$  with other parameters fixed. Finally, we generate MOSWACP instances of various sizes, 34, 84, 536, 101, 117, 45, 93, 64, 89, and 113, for the datasets C15, C21, J10, J12, J14, J16, J18, J20, M2, and R3.

### 5.2. Parameter tuning

We design experiments over the instances of dataset C15 to obtain a set of values for MOSWACP parameters and optimal parameters for the proposed ERSA using response surface methodology (RSM). The RSM is a statistical and mathematical technique widely employed in experimental design and optimization processes (Khuri and Mukhopadhyay, 2010). It is a powerful tool for understanding complex relationships between input factors and the response of a system. The RSM simultaneously explores the optimal settings for multiple parameters, leading to improved efficiency and performance of a given process or system (Campatelli et al., 2014). In this study, we input the parameters of ERSA and the instances of C15 to the RSM and determine optimal parameters according to the objective function values.

We illustrate the ranges and optimal values of the parameters obtained by ERSA in Fig. 9. Since the output of RSM for the parameters,  $N$ ,  $E_n^0$ ,  $CV$ , and  $M$  were float numbers, we rounded them to the nearest integer. Then, we found the best values for the parameters to minimize the objective function as  $N = 60$ ,  $\beta = 0.5$ ,  $E_n^0 = 1500$ ,  $CV = 50$ ,  $M = 3600$ , and  $r = 0.2$ . Also, Fig. A.1 (see Appendix A) shows the behavior of the objective function value,  $OF$  (represented on the y-axis), for different values of the parameters,  $N$ ,  $\beta$ ,  $E_n^0$ ,  $CV$ ,  $r$ , and  $M$  (represented on the x-axis). This figure shows that the objective function value negatively correlates with  $M$  and  $E_n^0$  but has no meaningful relationship with the remaining parameters. The objective function value in these experiments was the average of the objective function value of the first 10 instances of the C15 dataset returned by ERSA.

### 5.3. Solutions to the adopted MIP model

In this section, we solve MOSWACP at different sizes by the exact commercial solver, CPLEX, and illustrate computational results in Table 3.

Due to the execution time limit, we set it to one hour ( $T = 3600$  seconds), and left few instances from each dataset unsolved to optimality. As shown in the table, we solved all instances of the datasets C15 and J10 in about 18 and 1 minutes, respectively. Also, the MIP solver efficiently solves the instances of datasets C21, J12, J14, and J16 by obtaining optimal solutions in more than 90% of the instances. However, solving the instances of dataset J20 is challenging for CPLEX since only less than 60% of cases are solved optimally by CPLEX. On average, 88% of all instances are solved optimally by CPLEX in about 12 minutes.

---

<sup>2</sup>[http://www.om-db.wi.tum.de/psplib/getdata\\_mm.html](http://www.om-db.wi.tum.de/psplib/getdata_mm.html)

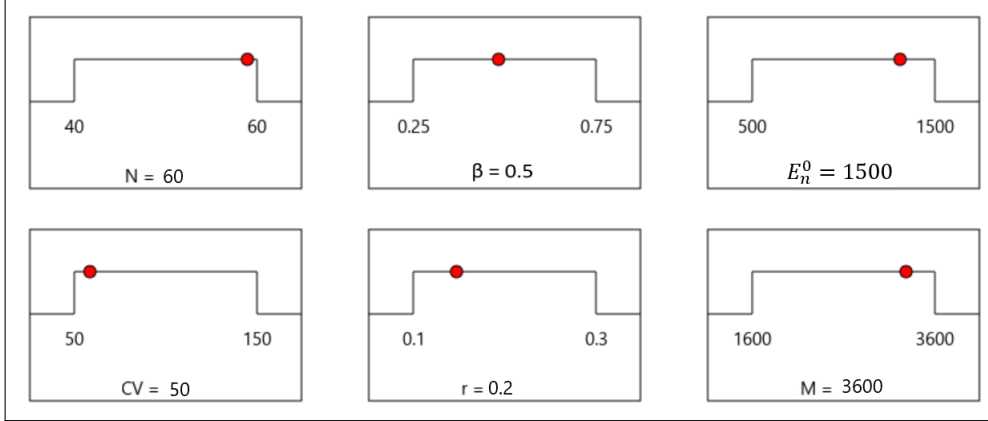


Figure 9: Best values of ERSA parameters for MOSWACP based on the dataset C15

Table 3: The computational results on different datasets of the MOSWACP instances solved by CPLEX ( $T$ : execution time in seconds)

Dataset	Minimum T	Maximum T	Average T	# executed instances	# instances solved optimally	% instances solved optimally
<i>C15</i>	5	2655	911	34	34	100
<i>C21</i>	15	3600	1100	84	77	92
<i>J10</i>	1	601	52	536	536	100
<i>J12</i>	1	3600	60	101	100	99
<i>J14</i>	4	3600	399	117	116	99
<i>J16</i>	5	3600	498	45	41	91
<i>J18</i>	5	3600	501	93	68	73
<i>J20</i>	22	3600	1991	64	37	58
<i>M2</i>	3	3600	770	89	75	84
<i>R3</i>	5	3600	801	113	95	84
<b>Average</b>	6.60	3205.60	708.30	—	—	88

#### 5.4. ERSA performance evaluation

In this section, we solve MOSWACP instances of different sizes using our proposed ERSA, equipped with improvement rules. Also, we compare the performance of the proposed ERSA with SA, GA, and PSO, as summarized in Table 4. We set the execution time limit to 1 minute in these experiments and obtain the optimal value of parameters by RSM (Dean et al., 2017). We put the parameters of GA to  $N = 50$ ,  $p_c = 0.3$ ,  $p_m = 0.2$ ,  $r_m = 0.2$ ,  $C_p = 0.2$ , where  $N$  is the population size,  $p_c$  is the crossover probability,  $p_m$  is the mutation probability,  $r_m$  is the mutation rate, and  $C_p$  is the crossover point. Also, we found optimal values for the SA parameters as  $T_{max} = 1000$ ,  $T_{min} = 0.01$ ,  $\alpha = 0.98$ ,  $N = 20$ , where  $\alpha$  is the cooling rate, and  $N$  is the number of iterations at each temperature. We also set the parameters of PSO to  $n_s = 20$ ,  $M = 100$ , and  $c_1 = c_2 = 2$ , where  $n_s$  denotes the size of the swarm,  $M$  is the maximum number of iterations. Also,  $c_1$  and  $c_2$  are the learning factors.

In Table 4, we illustrate 5 different versions of ERSA equipped with a different set of improvement rules involved: (i) ERSA with no improvement rule,  $ERSA_0$ ; (ii) ERSA with all improvement rules except  $IR_3$ ,  $ERSA_1$ ; (iii) ERSA with all improvement rules except  $IR_2$ ,  $ERSA_2$ ; (iv) ERSA with all improvement rules except  $IR_1$ ,  $ERSA_3$ ; and (v) ERSA with all improvement rules,  $ERSA_4$ . Also, we compare metaheuristic solvers according to three different criteria: (i)  $N^*$ , the number of instances solved to optimality; (ii)  $R^*$ , the average

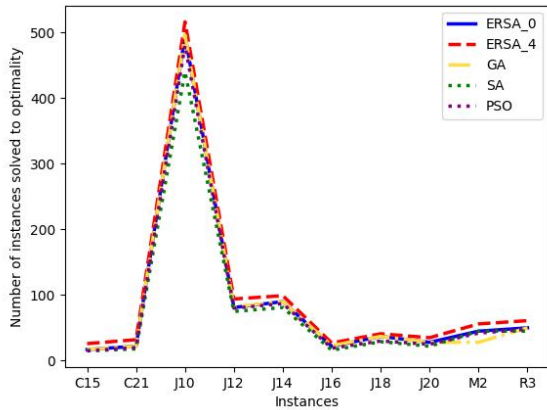
of relative percentage between the best-found solutions,  $f$  (returned by metaheuristics), and the optimal solutions,  $f^*$  (returned by MIP solver), where  $R^* = \frac{f-f^*}{f^*} * 100$ ; and (iii)  $T^*$ , the average execution time. As shown in Table 4, our proposed  $ERSA$  with the proposed improvement rules performs better than existing metaheuristic solvers in terms of the number of instances solved to optimality and the average gap between the best-found and optimal solutions. Moreover, the designed improvement rules are superior to the solvers regarding solution quality and closeness to the optimal solution. We compare the proposed  $ERSA$  with the existing metaheuristic solvers in terms of the number of instances solved to optimality,  $N^*$ , as well as the average of relative percentage between the best-found solution and the optimal solution,  $R^*$ , in Fig. 10. The result reveals that the proposed  $ERSA$  bundled with improvement rules,  $ERSA_4$ , has a better performance compared to the existing metaheuristic solvers.

Table 4: The comparison of the proposed  $ERSA$  with the existing metaheuristics at various-sized instances of MOSWACP

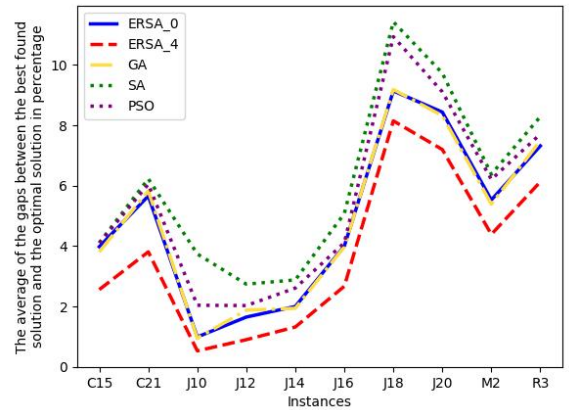
Dataset	# instances	Criteria	$ERSA_0$	$ERSA_1$	$ERSA_2$	$ERSA_3$	$ERSA_4$	GA	SA	PSO
<i>C15</i>	34	$N^*$	17	20	21	21	26	17	15	15
		$R^*$	3.98	3.74	3.72	3.24	2.56	3.81	4.11	4.10
		$T^*$	31.09	35.55	36.13	39.15	43.19	39.01	45.11	36.09
<i>C21</i>	84	$N^*$	22	25	26	26	32	22	18	20
		$R^*$	5.66	5.34	5.33	5.21	3.81	5.83	6.23	6.05
		$T^*$	41.66	45.08	49.01	51.00	55.01	49.22	48.01	50.17
<i>J10</i>	536	$N^*$	495	499	501	501	516	496	440	480
		$R^*$	0.99	0.83	0.81	0.80	0.53	0.95	3.74	2.04
		$T^*$	37.66	39.01	44.43	45.81	49.01	44.82	48.00	49.76
<i>J12</i>	101	$N^*$	81	85	87	87	94	82	75	80
		$R^*$	1.65	1.50	1.32	1.12	0.90	1.88	2.74	2.03
		$T^*$	39.01	42.01	44.91	45.09	49.33	44.10	42.04	47.16
<i>J14</i>	117	$N^*$	90	94	94	95	99	90	81	87
		$R^*$	2.00	1.78	1.50	1.45	1.32	1.94	2.88	2.61
		$T^*$	44.09	46.12	48.01	49.12	50.81	49.66	45.08	51.00
<i>J16</i>	45	$N^*$	22	22	23	25	27	23	16	19
		$R^*$	4.00	3.41	3.30	3.01	2.67	3.98	5.08	4.11
		$T^*$	41.33	42.01	45.39	46.91	49.11	51.60	50.44	51.05
<i>J18</i>	93	$N^*$	37	37	38	38	41	37	29	30
		$R^*$	9.14	8.21	8.20	8.18	8.15	9.19	11.43	10.94
		$T^*$	49.12	49.44	49.31	49.91	50.09	54.80	45.04	50.77
<i>J20</i>	64	$N^*$	28	28	29	33	35	28	22	25
		$R^*$	8.44	8.09	7.91	7.53	7.20	8.32	9.73	9.11
		$T^*$	42.22	43.01	45.90	47.38	49.00	49.32	44.01	48.71
<i>M2</i>	89	$N^*$	45	48	50	54	56	28	45	42
		$R^*$	5.53	5.31	5.02	4.66	4.39	5.39	6.38	6.21
		$T^*$	42.06	45.71	46.03	48.91	50.33	56.81	42.01	48.97
<i>R3</i>	113	$N^*$	50	53	55	58	61	50	45	48
		$R^*$	7.32	7.01	6.95	6.61	6.13	7.49	8.29	7.71
		$T^*$	46.11	48.64	48.93	48.99	52.94	55.99	49.22	53.01

Also, we compare the fraction of the total instances solved to the optimality of each dataset. As shown in Fig. 11, the cases solved optimally in each dataset are highlighted in blue, and those not solved optimally are shaded in red. The prominent blue areas in these figures demonstrate the enhanced  $ERSA$ , incorporating the proposed improvement rules and finding relatively better optimal solutions compared to the existing solvers.

Also, we compare the convergence of  $ERSA_4$  with the other solvers in Fig. 12 for large instances of datasets *C21*, *J20*, *M2*, and *R3*, respectively. Even though GA outperforms PSO and SA in finding relatively better solutions on average, our proposed  $ERSA_4$  generates relatively higher-quality solutions. It searches for neighbor solutions more efficiently for large instances of MOSWACP. These figures illustrate that  $ERSA_4$  finds high-quality solutions in



(a) The comparison of  $N^*$



(b) The comparison of  $R^*$

Figure 10: The comparison of the enhanced ERSA with the existing solvers based on: (a)  $N^*$ , total instances solved to optimality, and (b)  $R^*$ , average of relative percentage between the best-found solutions

relatively earlier iterations and searches local solutions more efficiently than other methods.

Finally, we compare  $ERSA_4$  with the CPLEX solver in the last instance of each dataset. As given in Table 5, the proposed  $ERSA_4$  reaches optimality in 2 of datasets. Although the solutions by the CPLEX solver are acquired in one hour (3600 seconds), the proposed algorithm found solutions close to CPLEX solutions in approximately one minute (60 seconds) on average. Also, the gap, defined as the relative difference between the best-found solution by CPLEX and the proposed  $ERSA_4$ , depicts a faster performance of  $ERSA_4$  for large instances of datasets compared to the CPLEX.

Table 5: Comparison of CPLEX and  $ERSA_4$

Dataset	CPLEX			$ERSA_4$		
	Best-found solution	T	Optimal	Best-found solution	T	Gap (%)
<i>C15</i>	103.45	2655	Yes	103.45	63.64	0.00
<i>C21</i>	280.98	3600	No	284.43	61.44	1.23
<i>J10</i>	43.38	601	Yes	43.38	59.43	0.00
<i>J12</i>	49.51	3600	NO	49.54	60.94	0.06
<i>J14</i>	57.74	3600	NO	58.43	60.54	1.19
<i>J16</i>	61.99	3600	NO	64.98	62.81	4.82
<i>J18</i>	71.04	3600	NO	75.23	62.65	5.90
<i>J20</i>	85.44	3600	NO	88.49	63.28	3.57
<i>M2</i>	90.43	3600	NO	92.64	63.88	2.44
<i>R3</i>	102.47	3600	NO	107.82	62.91	5.22
<b>Average</b>	94.643	3205.6		96.839	62.15	2.44

The computational results demonstrate that our proposed Electron Radar Search Algorithm (ERSA) with all improvement rules outperforms the existing metaheuristics, achieving more instances solved to optimality and maintaining smaller gaps between the best-found solutions and optimal counterparts. Furthermore, the results highlight the effectiveness of the improvement rules compared to other solvers lacking enhancements, such as solution quality and proximity to the optimal solution.

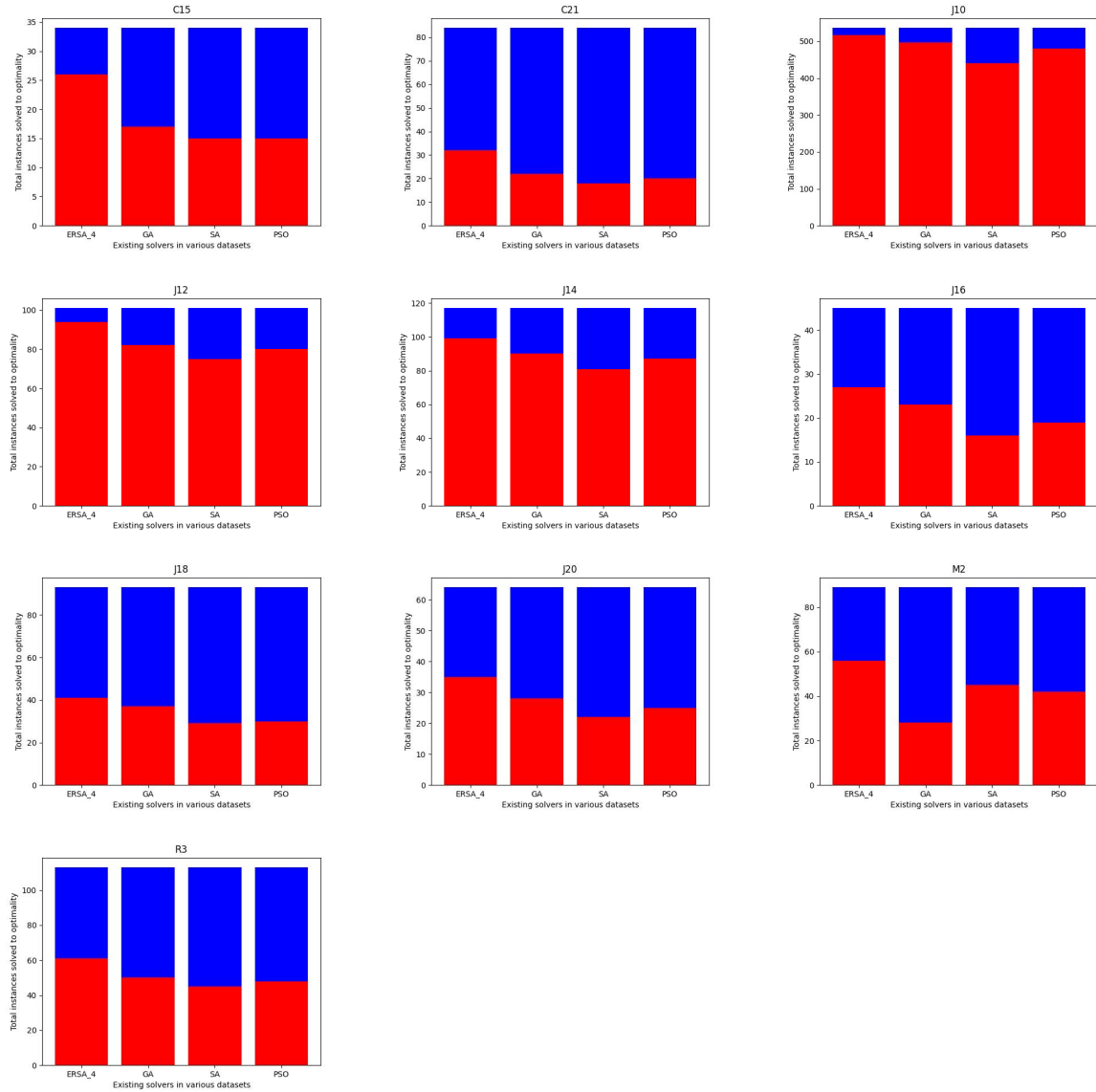
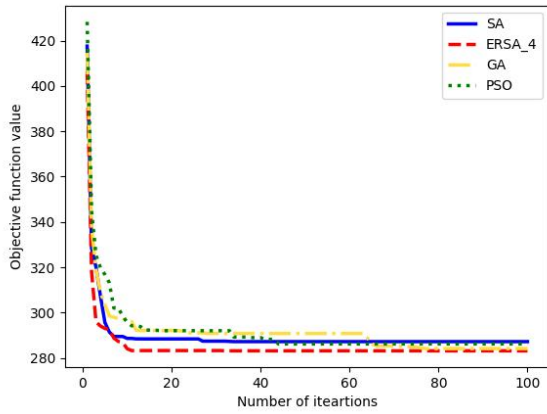
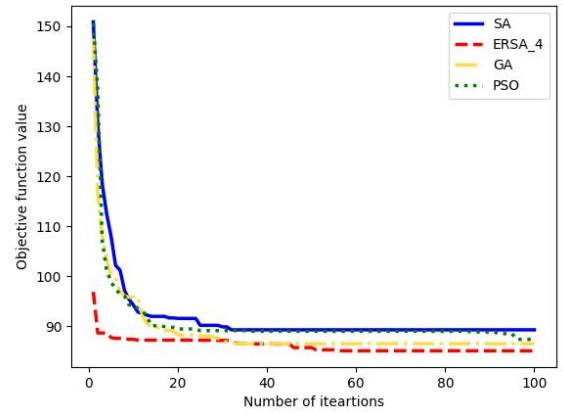


Figure 11: The number of instances solved (blue) and not solved (red) to optimality in datasets

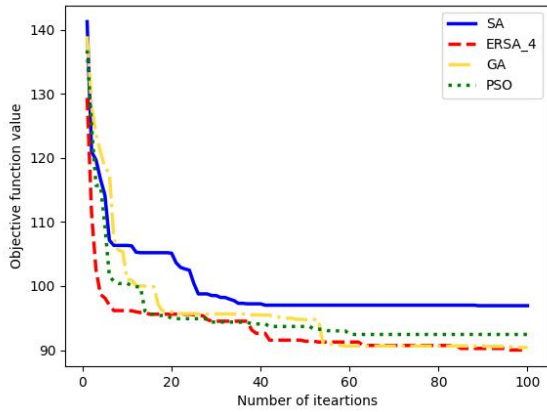
Moreover, the parameter of the spatial capacity of the construction site (denoted by  $Q$ ) is changed to observe its impact on the objective function. The ten instances of dataset C15 were selected, and the average objective function over these instances was reported. Fig. 13 shows the impact of changing the capacity of the construction/production site on the objective function (minimizing the usage cost of OSWs). As observed, the average cost is reducing (improving) by increasing the site's capacity ( $Q$ ). The reason is that by providing more capacity for a construction site, the OSWs could be installed anytime. So, the associated activities could utilize these OSWs, leading to lower makespan and efficient utilization of OSWs. Also, in lower capacities, the marginal impact is higher; however, after some point, increasing the capacity does not change the usage cost of OSWs. Therefore, the project managers must know that the larger site's capacity does not constantly improve the



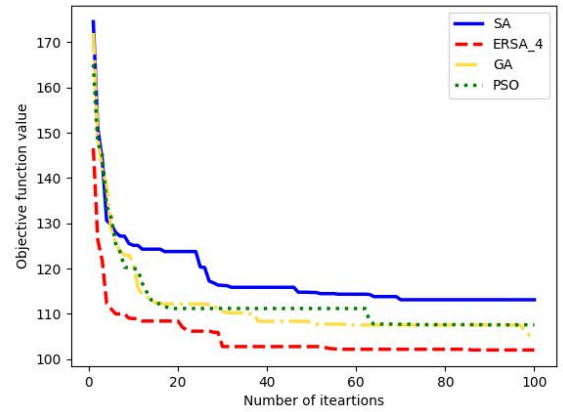
(a) C21



(b) J20



(c) M2



(d) R3

Figure 12: convergence history of  $ERSA_4$ , GA, PSO, and SA for instances of the datasets: (a) C21, (b) J20, (c) M2, and (d) R3

costs, and the optimal value of the  $Q$  could be found when the costs change drastically.

### 5.5. Case study

This section presents the application of the OSWs and their practicability for an actual case study related to a trailer production project. In this case study, we aim to locate the OSWs within the production site (considering the occupied space and their lifetime) to make the project scheduling more efficient and to utilize the resources more effectively, compared to traditional policies. Detailed information on the company is confidential upon their request. Since 2000, the company has expanded production lines, parts making, and assembly to more than 30,000 square meters of land. Data from the case study may be available upon a reasonable request and owner's permission. The information on project activities, duration, and precedence relations related to this project of the trailer production line is shown in Table 6. Also, the parameters related to the OSWs and storage areas within the manufacturing site are shown in Table 7.

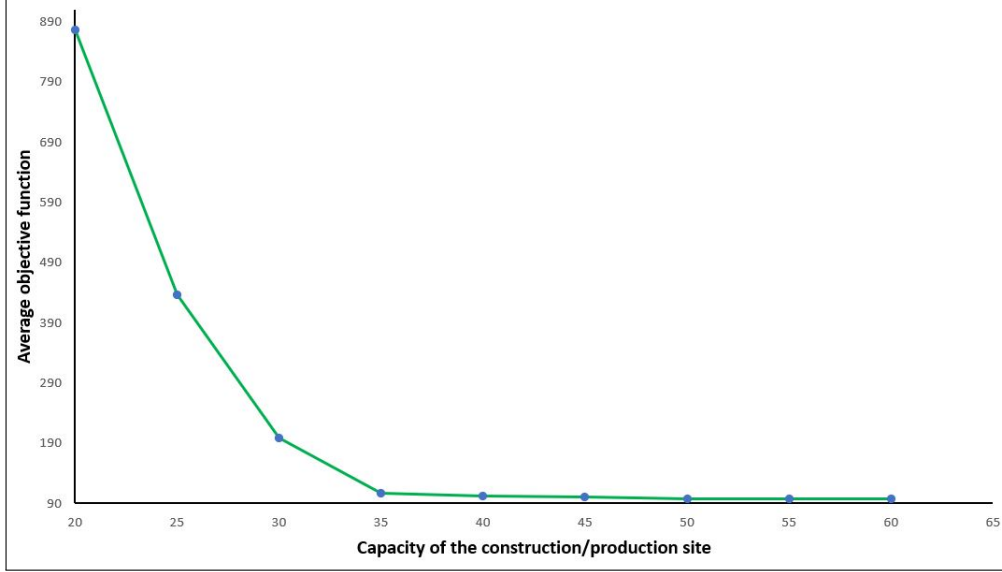


Figure 13: Impact of project's site capacity ( $Q$ ) on the usage cost of OSWs

Table 6: Activities, their duration and precedence relations in the case study

Activity	Duration (days)	Predecessors
A1	8	-
A2	5	A1
A3	7	A1
A4	6	A2, A3
A5	10	A4
A6	5	A4
A7	12	A5, A6
A8	8	A7

Table 7: OSWs, their duration and precedence relations in the case study

OSW	Cost per day (USD)	Installation Time (days)	Dismantling Time (days)	Space Occupied (units)	Max Lifetime (days)
W1	300	2	1	1	30
W2	400	3	2	1	40
W3	250	1	1	2	20

The project duration (deadline) is 50 days, with a total of eight activities (A1-A8) and three On-Site Workshops (W1-W3). The space limitation is two OSWs at a time. Also, OSWs must not exceed their maximum lifetime on-site. The project's purpose is to minimize total cost, which includes the cost of OSW availability while finding the installation and dismantling time of OSWs and the schedule of activities. Also, in the case study, one execution mode is considered for each activity. Also, the space occupied by each activity is assumed to be the same considering execution mode or OSW. The definition of each activity in the case study is stated as follows:

I **A1: Chassis Preparation.** This is the initial phase where the trailer chassis (the base frame) is assembled. This involves cutting, welding, and assembling steel beams

to create the skeleton of the trailer.

- II **A2: Axle and Suspension Installation.** Once the chassis is ready, the axles and suspension system are installed. These components ensure that the trailer can bear weight and move smoothly. Its predecessor is A1 (Chassis Preparation).
- III **A3: Wiring and Electrical Setup.** During this step, electrical wiring and systems are installed for brake lights, indicators, and internal electrical components. This includes routing cables along the chassis. Its predecessor is A1 (Chassis Preparation).
- IV **A4: Fabrication of Body Components.** The trailer body (e.g., side panels, floor, and roof) is fabricated and prepped. This involves metal cutting, shaping, and welding to create the trailer's exterior. Its predecessors are A2 (Axle and Suspension Installation), A3 (Wiring and Electrical Setup).
- V **A5: Paint and Surface Treatment.** The entire trailer chassis and body are primed, painted, and treated with anti-corrosion materials to ensure durability and resistance to weather conditions. Its predecessor is A4 (Fabrication of Body Components).
- VI **A6: Interior Fitting and Insulation.** Insulation materials and internal components (like partitions, insulation layers, or specialized fittings) are installed inside the trailer if required (for refrigerated or specialized trailers). Its predecessor is A4 (Fabrication of Body Components).
- VII **A7: Assembly of External Components.** This stage involves assembling external features such as doors, loading ramps, handles, and other accessories. Quality checks are also conducted at this stage. Its predecessors are A5 (Paint and Surface Treatment), A6 (Interior Fitting and Insulation).
- VIII **A8: Final Quality Control and Testing.** The trailer goes through final inspections, quality control checks, and testing (e.g., brake tests, durability tests, etc.) to ensure everything is functioning properly before delivery. Its predecessor is A7 (Assembly of External Components).

After solving the case study with our proposed methodology, the optimal activities' start and finish times were obtained as given in Table 8. Moreover, considering the spatial constraint (maximum of 2 OSWs installed at any time) and the lifetimes of the OSWs, the optimal schedule for OSW availability is shown in Table 9. According to the results, W1 is installed on Day 1 to handle initial activities like Chassis Preparation (A1) and Axle and Suspension Installation (A2). It also stays on-site until Day 26, covering the Interior Fitting (A6). W2 is installed on Day 16 to handle body fabrication and painting tasks like Fabrication of Body Components (A4) and Paint and Surface Treatment (A5). It remains on-site for 27 days until Day 43, when the Assembly of External Components (A7) is completed. W3 is installed on Day 32 to handle the final stages of assembly and Final Quality Control (A8), being dismantled after Day 50. Its availability is shorter, as it serves only during the final phase. The total usage cost for the OSWs is computed based on their availability times and per-day costs:

$$\text{W1 Cost: } 25 \text{ days} \times 300 \text{ USD/day} = 7,500 \text{ USD}$$

$$\text{W2 Cost: } 27 \text{ days} \times 400 \text{ SD/day} = 10,800 \text{ USD}$$



$$W3 \text{ Cost: } 18 \text{ days} \times 250 \text{ USD/day} = 4,500 \text{ USD}$$

Thus, the total OSW usage cost (objective function value) is:

$$\text{Total Cost} = 7,500 + 10,800 + 4,500 = 22,800 \text{ USD}$$

Activities' optimal start and finish times are provided, ensuring all precedence constraints are respected. The OSWs are optimally scheduled with installation and dismantling times to minimize costs while adhering to spatial constraints. The total usage cost of the OSWs (objective function) is 22,800 USD. This setup ensures that the resources are optimally allocated, minimizing the costs associated with the OSWs.

Table 8: Optimal schedule of activities

Activity	Duration (days)	Start Time (day)	Finish Time (day)
A1	8	Day 1	Day 8
A2	5	Day 9	Day 13
A3	7	Day 9	Day 15
A4	6	Day 16	Day 21
A5	10	Day 22	Day 31
A6	5	Day 22	Day 26
A7	12	Day 32	Day 43
A8	8	Day 44	Day 50

Table 9: Optimal installation and dismantling times of OSWs in the case study

OSW	Installation Time (day)	Dismantling Time (day)	Availability Duration (days)	Space Occupied (units)	Total Usage Cost (USD)
W1	Day 1	Day 26	25	1	$300 * 25 = 7,500$
W2	Day 16	Day 43	27	1	$400 * 27 = 10,800$
W3	Day 32	Day 50	18	2	$250 * 18 = 4,500$

In the following, we compare the total cost returned by our methodology with the total cost obtained by the traditional policies (based on past experiences). The activity's start and finish times and OSW's dismantling and installation time returned by the conventional policy are in Tables 10-11, respectively. Based on these tables, the total usage cost of OSWs when using traditional policy equals  $9,000 + 16,800 + 8,750 = 34,550$  USD. Compared with the optimal solution (22,800 USD), the savings with the Optimal Solution equal  $34,550 - 22,800 = 11,750$  USD. So, the optimal solution is 33.99% cheaper than the traditional approach. The reason is that in the optimal solution, the installation and dismantling of OSWs are timed more efficiently, reducing idle times. On the other hand, in the traditional solution, the OSWs are installed too early and kept for too long, which leads to unnecessarily higher usage costs.

Furthermore, the optimal solution respects the space constraint by installing only two OSWs simultaneously, ensuring minimal overlap and avoiding resource congestion. The solution using traditional policy doesn't fully account for space optimization. Although it respects the constraint, the inefficiency in scheduling leads to wasted space, as some OSWs remain idle for extended periods. Also, the optimal solution leverages more precise timing of the availability of OSWs, coordinating their use exactly when needed and dismantling them

Table 10: The start and finish times of activities in the case study using traditional policy

Activity	Duration (days)	Start Time (day)	Finish Time (day)
A1	8	Day 1	Day 8
A2	5	Day 9	Day 13
A3	7	Day 9	Day 15
A4	6	Day 16	Day 21
A5	10	Day 22	Day 31
A6	5	Day 22	Day 26
A7	12	Day 32	Day 43
A8	8	Day 44	Day 50

Table 11: The installation and dismantling times of OSWs in the case study using traditional policy

OSW	Installation Time (day)	Dismantling Time (day)	Availability Duration (days)	Space Occupied (units)	Total Usage Cost (USD)
W1	Day 1	Day 31	30	1	300 * 30 = 9,000
W2	Day 1	Day 43	42	1	400 * 42 = 16,800
W3	Day 16	Day 50	35	2	250 * 35 = 8,750

when their role is complete. In contrast, the traditional solution installs OSWs too early and dismantles them too late, resulting in longer usage durations and higher costs.

In addition, in the optimal solution, OSWs are scheduled to avoid idle periods, ensuring they are only used when necessary for the associated activities. The traditional solution, however, leads to extended periods where OSWs are idle, occupying space but not contributing to the project, leading to unnecessary costs. Regarding cost efficiency, the optimal solution minimizes the number of days that OSWs are in use, resulting in a significant cost reduction. In the traditional solution, the usage periods are excessive, inflating the cost by nearly 12,000 USD.

## 6. Discussion and Conclusion

When we compare *ERSA* with improvement rules (*ERSA<sub>4</sub>*) to the existing metaheuristic solvers using two metrics, namely  $N^*$  (total instances solved to optimality) and  $R^*$  (the average difference (relative percentage) between the best-found solution and the optimal solution), the *ERSA<sub>4</sub>* exhibits superior efficiency. One notable strength of *ERSA<sub>4</sub>* is the rapid convergence to the best-found solution in early iterations, which sets it apart from alternative methods. The *ERSA* excels at generating and exploring neighboring solutions, ultimately leading to the exploration of high-quality solutions. With large instances of MOSWACP, the Genetic Algorithm (GA) outperforms Particle Swarm Optimization (PSO) and Simulated Annealing (SA). GA consistently achieves solutions with lower objective function values, indicating its prowess in finding superior solutions.

Moreover, as we compared the solutions generated by the CPLEX solver and *ERSA<sub>4</sub>*, our proposed algorithm achieves optimal solutions in 2 datasets and, on average, reaches the solutions close to CPLEX solutions in 8 other instances by approximately 2.34%. This paper adopted the project resource cost availability problem with OSWs and multi-mode activities, a mixed-integer programming model (Moradi et al., 2023). We developed a model-specific Electron Radar Search Algorithm (ERSA) with purposeful improvement rules to solve large-scale MOSWACP. The proposed method consistently outperforms other metaheuristic solvers by achieving relatively high-quality solutions and maintaining smaller gaps between the

best-found and optimal solutions, specifically in early iterations in relatively short times. An actual case study related to the trailer production site was solved by the proposed methodology. The optimal solution was significantly better due to its focus on timing and efficient resource management. It resulted in 11,750 USD in savings (a 33.99% reduction in costs) compared to traditional policies. This highlights the importance of optimization in resource allocation and scheduling, which is achieved effectively using the proposed model.

For future direction, we recommend focusing on the location of workshops since their neighborhood and other resources might matter in real-world practices. Also, MOSWACP, with material procurement limitations, is a potential opportunity to develop. We also suggest extending existing metaheuristics to solve MOSWACP and comparing them with benchmark solvers. Also, uncertain and stochastic parameters related to resource availability could be addressed by agent-based simulation models (Aftabi et al., 2025). Such exploration helps the construction industry deploy superior methods to schedule projects optimally and use large-scale solvers for project initiatives.

### **Consent for publication**

All authors consent to the publication. All authors read and approved the final manuscript.

### **Funding**

The authors received no financial support for this paper's research, authorship, and publication.

### **Data Availability Statement**

Data, models, and codes are available upon request.

### **Conflict of interest**

The authors have no conflicts of interest to disclose.

### **Acknowledgements**

Not applicable.

### **References**

- Afshar-Nadjafi, B., 2014a. Multi-mode resource availability cost problem with recruitment and release dates for resources. *Applied Mathematical Modelling* 38, 5347–5355.
- Afshar-Nadjafi, B., 2014b. Using grasp for resource availability cost problem with time dependent resource cost. *Economic Computation & Economic Cybernetics Studies & Research* 48.

- Afshar-Nadjafi, B., Basati, M., Maghsoudlou, H., 2017. Project scheduling for minimizing temporary availability cost of rental resources and tardiness penalty of activities. *Applied Soft Computing* 61, 536–548.
- Aftabi, N., Moradi, N., Mahroo, F., Kianfar, F., 2025. Sd-abm-ism: An integrated system dynamics and agent-based modeling framework for information security management in complex information systems with multi-actor threat dynamics. *Expert Systems with Applications* 263, 125681.
- Alcaraz, J., Maroto, C., Ruiz, R., 2003. Solving the multi-mode resource-constrained project scheduling problem with genetic algorithms. *Journal of the Operational Research Society* 54, 614–626.
- Arjmand, M., Najafi, A.A., Ebrahimzadeh, M., 2020. Evolutionary algorithms for multi-objective stochastic resource availability cost problem. *OPSEARCH* 57, 935–985.
- Böttcher, J., Drexl, A., Kolisch, R., Salewski, F., 1999. Project scheduling under partially renewable resource constraints. *Management Science* 45, 543–559.
- Brucker, P., Drexl, A., Möhring, R., Neumann, K., Pesch, E., 1999. Resource-constrained project scheduling: Notation, classification, models, and methods. *European Journal of Operational Research* 112, 3–41.
- Campatelli, G., Lorenzini, L., Scippa, A., 2014. Optimization of process parameters using a response surface method for minimizing power consumption in the milling of carbon steel. *Journal of cleaner production* 66, 309–316.
- Chen, L., Li, X., Cai, Z., 2012. Heuristic methods for minimizing resource availability costs in multi-mode project scheduling, in: 2012 IEEE International Conference on Systems, Man, and Cybernetics (SMC), IEEE. pp. 809–813.
- CPLEX, I., 2023. IBM ILOG CPLEX Optimizer. <https://www.ibm.com/products/ilog-cplex-optimization-studio/cplex-optimizer>. Accessed: 2023-03-20.
- De Reyck, B., Herroelen, W., 1999. The multi-mode resource-constrained project scheduling problem with generalized precedence relations. *European Journal of Operational Research* 119, 538–556.
- Dean, A., Voss, D., Draguljić, D., Dean, A., Voss, D., Draguljić, D., 2017. Response surface methodology. *Design and analysis of experiments* , 565–614.
- Deblaere, F., Demeulemeester, E., Herroelen, W., 2011. Proactive policies for the stochastic resource-constrained project scheduling problem. *European Journal of Operational Research* 214, 308–316.
- Demeulemeester, E.L., Herroelen, W.S., 2006. Project scheduling: a research handbook. volume 49. Springer Science & Business Media.

- Drexl, A., Gruenewald, J., 1993. Nonpreemptive multi-mode resource-constrained project scheduling. *IIE transactions* 25, 74–81.
- Drexl, A., Kimms, A., 2001. Optimization guided lower and upper bounds for the resource investment problem. *Journal of the Operational Research Society* 52, 340–351.
- Gerhards, P., 2020. The multi-mode resource investment problem: a benchmark library and a computational study of lower and upper bounds. *OR spectrum* 42, 901–933.
- Gerhards, P., Stürck, C., 2018. A hybrid metaheuristic for the multi-mode resource investment problem with tardiness penalty, in: *Operations Research Proceedings 2016*. Springer, pp. 515–520.
- GlobalKnowledge.com, 2020. Accessed 20 october 2020. <https://www.globalknowledge.com/ca-en/resources/resource-library/articles/importance-of-project-schedule-and-cost-control-in-project-management>.
- Guldemon, T., Hurink, J.L., Paulus, J.J., Schutten, J.M., 2008. Time-constrained project scheduling. *Journal of Scheduling* 11, 137–148.
- Hartmann, S., Briskorn, D., 2022. An updated survey of variants and extensions of the resource-constrained project scheduling problem. *European Journal of Operational Research* 297, 1–14.
- Herroelen, W., 2005. Project scheduling—theory and practice. *Production and Operations Management* 14, 413–432.
- Herroelen, W., De Reyck, B., Demeulemeester, E., 1998. Resource-constrained project scheduling: A survey of recent developments. *Computers & Operations Research* 25, 279–302.
- Hsu, C.C., Kim, D.S., 2005. A new heuristic for the multi-mode resource investment problem. *Journal of the Operational Research Society* 56, 406–413.
- Javanmard, S., Afshar-Nadjafi, B., Niaki, S.T.A., 2017. Preemptive multi-skilled resource investment project scheduling problem: Mathematical modelling and solution approaches. *Computers & Chemical Engineering* 96, 55–68.
- Kayvanfar, V., Zandieh, M., Arashpour, M., 2023. Hybrid bi-objective economic lot scheduling problem with feasible production plan equipped with an efficient adjunct search technique. *International Journal of Systems Science: Operations & Logistics* 10, 2059721.
- Khuri, A.I., Mukhopadhyay, S., 2010. Response surface methodology. *Wiley Interdisciplinary Reviews: Computational Statistics* 2, 128–149.
- Kreter, S., Schutt, A., Stuckey, P.J., Zimmermann, J., 2018. Mixed-integer linear programming and constraint programming formulations for solving resource availability cost problems. *European Journal of Operational Research* 266, 472–486.

- Lambrechts, O., Demeulemeester, E., Herroelen, W., 2008. Proactive and reactive strategies for resource-constrained project scheduling with uncertain resource availabilities. *Journal of scheduling* 11, 121–136.
- Lu, Z., Ren, Y., Wang, L., Zhu, H., 2019. A resource investment problem based on project splitting with time windows for aircraft moving assembly line. *Computers & Industrial Engineering* 135, 568–581.
- Meng, H., Wang, B., Nie, Y., Xia, X., Zhang, X., 2016. A scatter search hybrid algorithm for resource availability cost problem, in: *Harmony Search Algorithm*. Springer, pp. 39–51.
- Moradi, N., Kayvanfar, V., Baldacci, R., 2023. On-site workshop investment problem: A novel mathematical approach and solution procedure. *Heliyon* .
- Moradi, N., Kayvanfar, V., Rafiee, M., 2022. An efficient population-based simulated annealing algorithm for 0–1 knapsack problem. *Engineering with Computers* 38, 2771–2790.
- Moradi, N., Shadrokh, S., 2019. Simultaneous solution of material procurement scheduling and material allocation to warehouse using simulated annealing. *Journal of Applied Research on Industrial Engineering* 6, 1–15.
- Naber, A., Kolisch, R., 2014. Mip models for resource-constrained project scheduling with flexible resource profiles. *European Journal of Operational Research* 239, 335–348.
- Najafi, A.A., Niaki, S.T.A., 2006. A genetic algorithm for resource investment problem with discounted cash flows. *Applied Mathematics and Computation* 183, 1057–1070.
- Najafi, A.A., Niaki, S.T.A., Shahsavar, M., 2009. A parameter-tuned genetic algorithm for the resource investment problem with discounted cash flows and generalized precedence relations. *Computers & Operations Research* 36, 2994–3001.
- Pellerin, R., Perrier, N., Berthaut, F., 2020. A survey of hybrid metaheuristics for the resource-constrained project scheduling problem. *European Journal of Operational Research* 280, 395–416.
- Peteghem, V.V., Vanhoucke, M., 2015. Heuristic methods for the resource availability cost problem, in: *Handbook on Project Management and Scheduling Vol. 1*. Springer, pp. 339–359.
- Qi, J., Guo, B., Lei, H., Zhang, T., 2014. Solving resource availability cost problem in project scheduling by pseudo particle swarm optimization. *Journal of Systems Engineering and Electronics* 25, 69–76.
- Rahmanzadeh, S., Pishvaei, M.S., 2020. Electron radar search algorithm: a novel developed meta-heuristic algorithm. *Soft Computing* 24, 8443–8465.
- Ranjbar, M., Kianfar, F., Shadrokh, S., 2008. Solving the resource availability cost problem in project scheduling by path relinking and genetic algorithm. *Applied Mathematics and Computation* 196, 879–888.

- Rodrigues, S.B., Yamashita, D.S., 2010. An exact algorithm for minimizing resource availability costs in project scheduling. *European Journal of Operational Research* 206, 562–568.
- Rodrigues, S.B., Yamashita, D.S., 2015. Exact methods for the resource availability cost problem, in: *Handbook on Project Management and Scheduling Vol. 1*. Springer, pp. 319–338.
- Rose, C., Coenen, J., Hopman, H., 2016. Definition of ship outfitting scheduling as a resource availability cost problem and development of a heuristic solution technique. *Journal of Ship Production and Design* 32, 154–165.
- Shadrokh, S., Kianfar, F., 2007. A genetic algorithm for resource investment project scheduling problem, tardiness permitted with penalty. *European Journal of Operational Research* 181, 86–101.
- Shahsavar, A., Zoraghi, N., Abbasi, B., 2018. Integration of resource investment problem with quantity discount problem in material ordering for minimizing resource costs of projects. *Operational Research* 18, 315–342.
- Shahsavar, M., Niaki, S.T.A., Najafi, A.A., 2010. An efficient genetic algorithm to maximize net present value of project payments under inflation and bonus–penalty policy in resource investment problem. *Advances in Engineering Software* 41, 1023–1030.
- ShelterLogic, 2022. Accessed 26 december 2022. <https://www.shelterlogic.com/knowledge/site-workshops-storage-shelter-industry>.
- Su, C.T., Santoro, M.C., Mendes, A.B., 2018. Constructive heuristics for project scheduling resource availability cost problem with tardiness. *Journal of Construction Engineering and Management* 144, 04018074.
- Subulan, K., 2020. An interval-stochastic programming based approach for a fully uncertain multi-objective and multi-mode resource investment project scheduling problem with an application to erp project implementation. *Expert Systems with Applications* 149, 113189.
- Tian, B., Zhang, J., Demeulemeester, E., Chen, Z., Ali, H., 2023. Integrated resource-constrained project scheduling and material ordering problem with limited storage space. *Computers & Industrial Engineering* , 109608.
- Van Peteghem, V., Vanhoucke, M., 2010. A genetic algorithm for the preemptive and non-preemptive multi-mode resource-constrained project scheduling problem. *European Journal of Operational Research* 201, 409–418.
- Van Peteghem, V., Vanhoucke, M., 2012. An invasive weed optimization algorithm for the resource availability cost problem, in: *25th European conference on operational research (EURO XXV; EURO 2012)*.

- Van Peteghem, V., Vanhoucke, M., 2013. An artificial immune system algorithm for the resource availability cost problem. *Flexible Services and Manufacturing Journal* 25, 122–144.
- Viana, A., de Sousa, J.P., 2000. Using metaheuristics in multiobjective resource constrained project scheduling. *European Journal of Operational Research* 120, 359–374.
- Visual-Planning.com, 2020. Accessed 16 october 2022. <https://www.visual-planning.com/en/blog/construction-scheduling-software-why-is-scheduling-important-in-construction>.
- Yamashita, D.S., Armentano, V.A., Laguna, M., 2006. Scatter search for project scheduling with resource availability cost. *European Journal of Operational Research* 169, 623–637.
- Yamashita, D.S., Armentano, V.A., Laguna, M., 2007. Robust optimization models for project scheduling with resource availability cost. *Journal of scheduling* 10, 67–76.
- Yamashita, D.S., Morabito, R., et al., 2009. A note on time/cost tradeoff curve generation for project scheduling with multi-mode resource availability costs. *International Journal of Operational Research* 5, 429–444.
- Zhang, Y., Cui, N., 2021. Project scheduling and material ordering problem with storage space constraints. *Automation in Construction* 129, 103796.
- Zhu, X., Ruiz, R., Li, S., Li, X., 2017. An effective heuristic for project scheduling with resource availability cost. *European Journal of Operational Research* 257, 746–762.

## Appendix A. Objective function behavior with respect to ERSA parameters

Fig. A.1 illustrates how the objective function value (OF) changes at different values of the parameters,  $N$ ,  $\beta$ ,  $E_n^0$ ,  $CV$ ,  $r$ , and  $M$ , on the vertical and horizontal axis, respectively. The objective function value in these experiments is an average derived from ERSA’s first 10 instances of the dataset, C15.



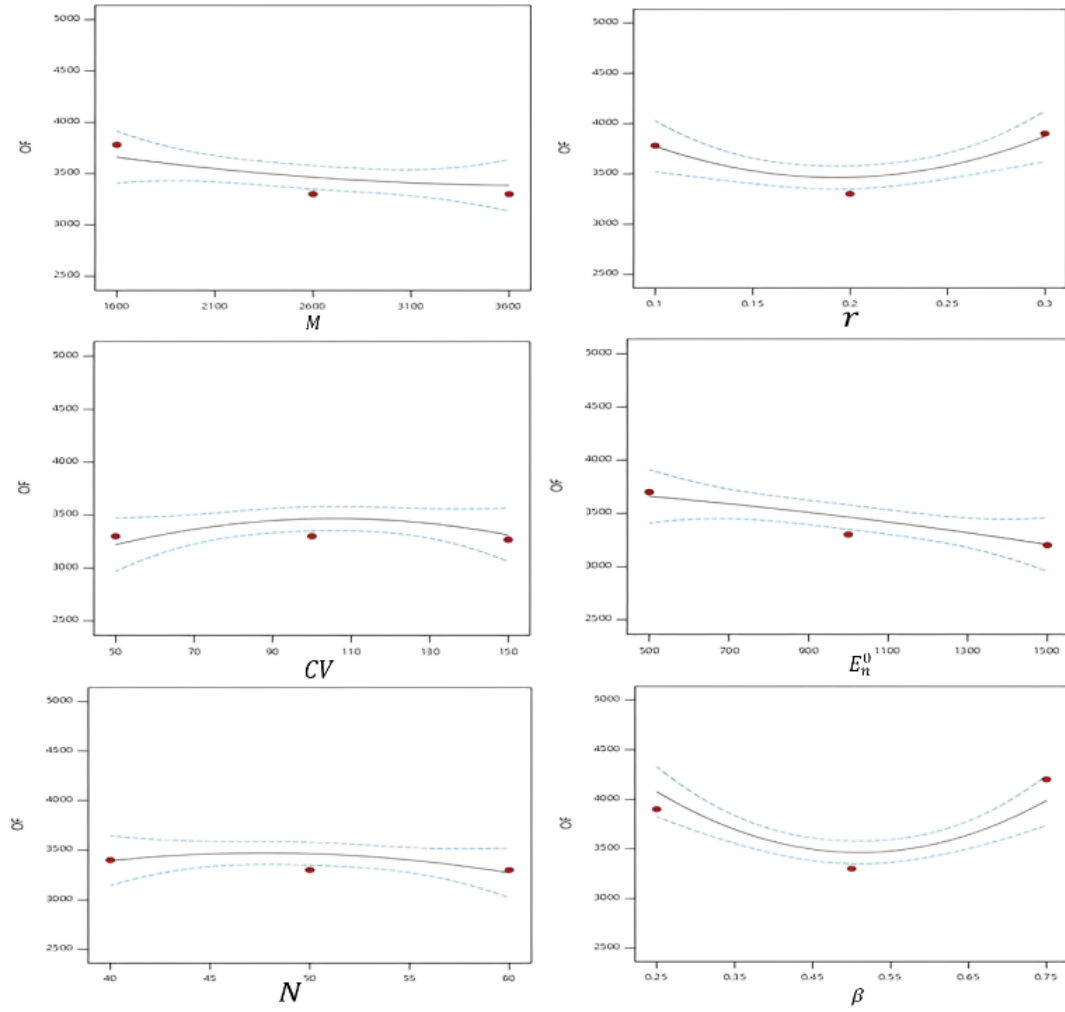


Figure A.1: The behavior of the objective function ( $OF$ ) with respect to the parameters of ERSA